Heikkinen, Ismo T. S.; Koutsourakis, George; Virtanen, Sauli; Yli-Koski, Marko; Wood, Sebastian; Vähänissi, Ville; Salmi, Emma; Castro, Fernando A.; Savin, Hele

AlOx surface passivation of black silicon by spatial ALD: Stability under light soaking and damp heat exposure

Published in:
JOURNAL OF VACUUM SCIENCE AND TECHNOLOGY A

DOI:
10.1116/1.5133896

Published: 01/03/2020

Document Version
Peer reviewed version

Please cite the original version:
Heikkinen, I. T. S., Koutsourakis, G., Virtanen, S., Yli-Koski, M., Wood, S., Vähänissi, V., Salmi, E., Castro, F. A., & Savin, H. (2020). AlOx surface passivation of black silicon by spatial ALD: Stability under light soaking and damp heat exposure. *JOURNAL OF VACUUM SCIENCE AND TECHNOLOGY A*, *38*(2), [022401]. https://doi.org/10.1116/1.5133896

The following article has been accepted by Journal of Vacuum Science & Technology A. After it is published, it will be found at https://avs.scitation.org/journal/jva.

AlO_x Surface Passivation of Black Silicon by Spatial ALD: Stability under Light Soaking and Damp Heat Exposure

Running title: AlO_x Surface Passivation of Black Silicon by Spatial ALD: Stability under Light Soaking and Damp Heat Exposure

Running Authors: Heikkinen *et al.*

Ismo T.S. Heikkinen[1,a)], George Koutsourakis[2], Sauli Virtanen[3], Marko Yli-Koski[1], Sebastian Wood[2], Ville Vähänissi[1], Emma Salmi[3], Fernando A. Castro[2], and Hele Savin[1]

[1]Aalto University, Department of Electronics and Nanoengineering, Tietotie 3, FI-02150, Espoo, Finland

[2]National Physical Laboratory, Hampton Road, Teddington, TW11 0LW, United Kingdom

[3]Beneq Oy, Olarinluoma 9, FI-02200, Espoo, Finland

[a)] Electronic mail: ismo.heikkinen@aalto.fi

Scientific breakthroughs in silicon surface passivation have enabled commercial high-efficiency photovoltaic devices making use of the black silicon nanostructure. In this study, we report on factors that influence the passivation stability of black silicon realized with industrially viable Spatial Atomic Layer Deposited (SALD) aluminum oxide (AlO_x) under damp heat exposure and light soaking. Damp heat exposure conditions are 85°C and 85% relative humidity, and light soaking is performed with 0.6 Sun illumination at 75°C. It is demonstrated that reasonably thick (20 nm) passivation films are required for both black and planar surfaces in order to provide stable surface

passivation over a period of 1000 h under both testing conditions. Both surface textures degrade at similar rates with 5 nm and 2 nm thick films. The degradation mechanism under damp heat exposure is found to be different from that in light soaking. During damp heat exposure, the fixed charge density of AlO_x is reduced, which decreases the amount of field-effect passivation. Degradation under light soaking, on the other hand, is likely to be related to interface defects between silicon and the passivating film. Finally, a thin chemically-grown SiO_x layer at the interface between the AlO_x film and the silicon surface is shown to significantly increase the passivation stability under both light soaking and damp heat exposure. The results of this study provide valuable insights on surface passivation degradation mechanisms on nanostructured silicon surfaces, and pave the way for the industrial production of highly stable black silicon devices.

Keywords: spatial atomic layer deposition; aluminum oxide; light soaking; damp heat exposure; surface passivation; charge carrier lifetime

I. INTRODUCTION

Nanostructured silicon (black silicon, b-Si) with its superb optical performance has emerged as an attractive surface texture for various photovoltaic (PV) applications. Examples of such devices include photodetectors with close to ideal response over a wide wavelength range[1] and high-efficiency solar cells[2]. The emergence of these devices is enabled by Atomic Layer Deposition (ALD), which is used to passivate the nanostructured surface with a thin dielectric layer, often aluminum oxide (AlO_x). The exceptional passivation performance achieved with ALD AlO_x is based on two aspects[3,4]: I) the low density of defects at the interface of silicon and the passivation film, and II) the high negative charge present in the film. ALD films are highly conformal, which makes

them the method of choice for b-Si passivation[5]. Furthermore, the b-Si morphology enhances the field-effect passivation provided by the negative fixed charge density[6]. Scientific progress on b-Si passivation has matured to the stage where commercial b-Si photovoltaic devices are emerging[7-11], making it important to consider how large-scale fabrication methods, such as industrially-proven spatial ALD (SALD)[12,13], affect the long-term performance and stability of such devices.

Typical environmental conditions that can alter the efficiency of optoelectronic devices are elevated temperature, intense illumination, and ambient moisture. In the case of silicon-based devices, the evolution of performance can be related either to the surface or to the bulk properties of the substrate. Recently, major research efforts have been directed towards understanding the bulk defects in silicon that are caused by illumination in elevated temperature, named light and elevated temperature induced degradation (LeTID) by Kersten *et al.*[14] However, in this paper we focus on the degradation of surface passivation under illumination, which also can affect the efficiency of Si devices significantly. Sperber *et al.* have reported on the surface-related degradation mechanisms in planar silicon under illumination and elevated temperature, referred to as light soaking in this article. They have showed that AlO_x-based dielectric passivation stacks can exhibit significant changes in surface passivation quality regardless of the surface cleaning method prior to film deposition[15]. They also determined that passivation instability is related to the reduction of film charge[16] and to defects with an asymmetric capture cross-section very close to the silicon surface[17]. However, Niewelt *et al.* have reported that AlO_x-based surface passivation can be stable under light soaking for up to 3700 h[18]. A recent study by Kim *et al.*[19] suggested that hydrogen released from the passivation film

during annealing can be involved in surface-related degradation, but the exact mechanisms are not yet fully understood.

Stability under elevated temperature and relative humidity, here referred to as damp heat exposure, is also vital for the performance of high-efficiency photovoltaic devices. Stress testing conditions according to the IEC 61215-1-1 standard for solar panels are 85°C with 85% relative humidity (RH) for up to 1000 h of exposure, and in these degradation tests, it is important to distinguish between different failure modes of the devices. For solar panels, the test at 85°C/85% RH usually provides information on the performance of moisture-protecting encapsulation of the panel. Photodetectors, on the other hand, can be used with little or no encapsulation to ensure a sensitive photoresponse, so the device itself is physically exposed to 85°C/85% RH. Therefore, testing the surface passivation properties of AlO_x under these harsh conditions is important in terms of device performance.

Liang *et al.* studied how damp heat exposure affected the surface passivation of silicon achieved with 20 nm thick AlO_x layers deposited by Plasma-Enhanced ALD (PEALD)[20,21]. They reported that while degradation was slow, the minority charge carrier lifetime in boron-doped Float Zone (FZ) silicon had decreased by a notable extent, approximately 15%, after a 230 h exposure to 85°C/85% RH. The degradation occurred due to the reduction of passivation layer charge, probably resulting from the formation of AlO(OH) when the AlO_x layer reacted with the water vapor. They also showed that 70 nm thick Plasma-Enhanced Chemical Vapor Deposited (PECVD) SiN_x capping layers could be used to prevent the degradation of passivation in these conditions. Black silicon photovoltaic devices usually have a bare AlO_x film on the light-absorbing side, as no

antireflection coatings are needed due to the high absorbance of b-Si. In this case, a SiN_x capping layer on top of AlO_x would lead to increased processing costs in addition to undesired absorption of light before reaching the surface of for example a detector, leading to decreased photoresponse.

All aforementioned studies were done on planar silicon and using conventional ALD based on sequential precursor pulses, whereas in this article we study how the increased surface area of b-Si affects the extent and the kinetics of the degradation. Furthermore, we investigate how the faster film growth achieved with SALD influences the film quality and thus the stability of AlO_x passivation under both light soaking and damp heat exposure. SALD has a higher deposition rate compared to pulsing ALD, but the film growth in SALD might be disturbed by precursor intermixing[22,23], leading to decreased film quality. Therefore, understanding the extent of effects induced by light, elevated temperature and moisture in SALD AlO_x-passivated nanostructured silicon is vital for the wide-scale application of such devices. Samples for stability testing were fabricated from both b-Si and reference planar FZ Si wafers by coating them with different thicknesses of SALD AlO_x, and the passivation quality was monitored during light soaking and damp heat exposure. Film charge and interfacial defect density were measured before and after exposure to provide potential explanations for differences in passivation stability. In addition, the effect of the interface between the Si surface and the passivation film was studied by comparing samples with different surface finishes prior to film deposition.

II. EXPERIMENTAL

100 mm Float Zone (FZ) Si wafers supplied by Topsil GlobalWafers A/S were used as the substrate material. The 280 µm thick, <100>-oriented wafers had been boron-doped to a specified resistivity in the range of 1 Ωcm to 5 Ωcm. Figure 1 summarizes the process flow for sample fabrication, experiments, and characterization in this study. After cleaning the wafers with RCA solutions and dilute hydrofluoric acid (HF), the samples were annealed in an oxygen ambient at 1050°C for 30 min to deactivate intrinsic defects that can be detrimental for bulk lifetime in FZ Si. The elimination of the defects is described in detail by Grant *et al.*[24] The resulting thermally grown SiO_2 was removed from the wafers with 10% HF, after which the b-Si nanostructure was etched into selected wafers using cryogenic deep reactive ion etching (ICP-RIE) with parameters reported in[5]. An SEM image of the resulting b-Si nanostructure is shown in Figure 2. Wafers with the planar surface acted as reference samples to assess the effect of the b-Si texture on the degradation process. Prior to surface passivation with SALD AlO_x, both b-Si and planar wafers were treated with an RCA2 solution, which produced a thin, hydrogen-rich chemical silicon oxide (SiO_x) layer on the wafers. Additionally, instead of an RCA2 treatment, a few of the planar wafers were dipped in dilute HF prior to film deposition to remove any interfacial oxide. The difference in the resulting surface finish on Si wafers after these two chemical treatments is described by Green *et al.*[25] Here, the two different surface finishes were used to study the impact of the interfacial layer between Si and AlO_x on the stability of surface passivation.

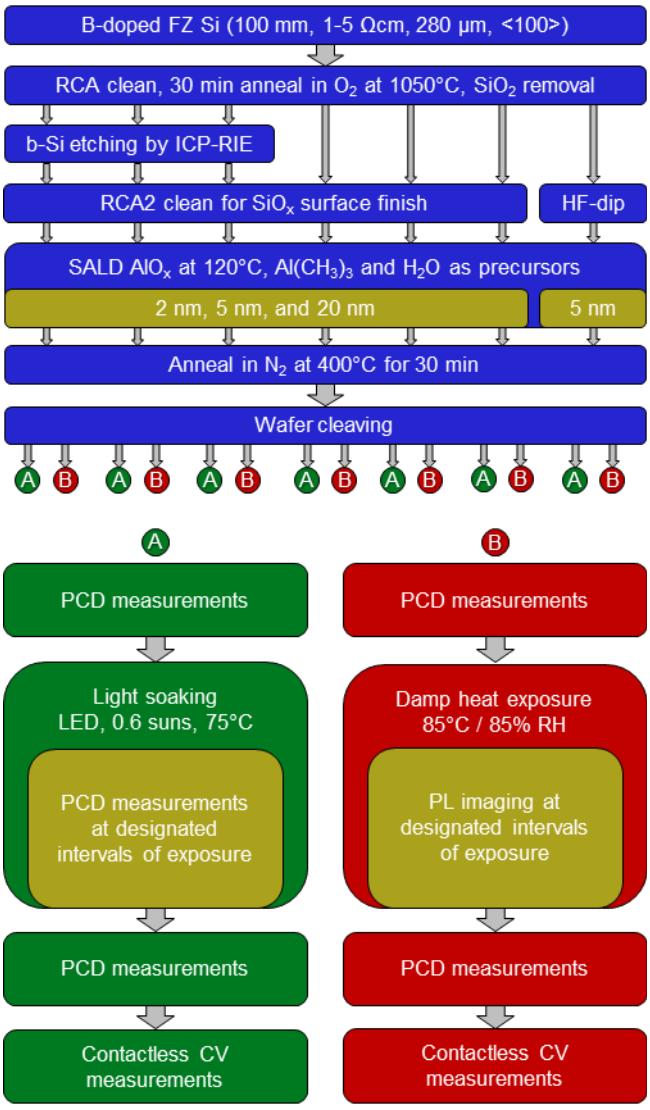

FIG. 1. Process flow describing sample fabrication, experimental procedures, and characterization methods for light soaking (A) and damp heat exposure (B).

A Beneq SCS 1000 SALD tool was used to coat the samples with AlO_x using $Al(CH_3)_3$ and H_2O as precursors. The surface passivation of black silicon using this tool and process has been demonstrated earlier[26]. Depositions were carried out at 120°C with a 4.5 m/min line speed, yielding a deposition rate of 2.6 nm/min. The SiO_x finished b-Si and planar wafers were coated with 2 nm, 5 nm and 20 nm thick AlO_x films, while the HF-dipped planar wafers were coated with 5 nm AlO_x. Two wafers of each type were

coated with the aforementioned films. After deposition the wafers were annealed in a N_2 environment at 400°C for 30 min to activate the surface passivation. Finally, the wafers were cleaved into quarters.

The effective minority charge carrier lifetime τ_{eff} was measured from the quarters before and after the stability experiments with the photoconductance decay (PCD) method[27] using a Sinton Instruments WCT-120 instrument. Each sample was measured with both generalized and transient modes. For high-lifetime samples ($\tau_{eff} \geq 800$ µs) the transient results were used in the analysis, while for samples with lower lifetime the generalized lifetimes were considered throughout the experiments. This was done to ensure the comparability of the results.

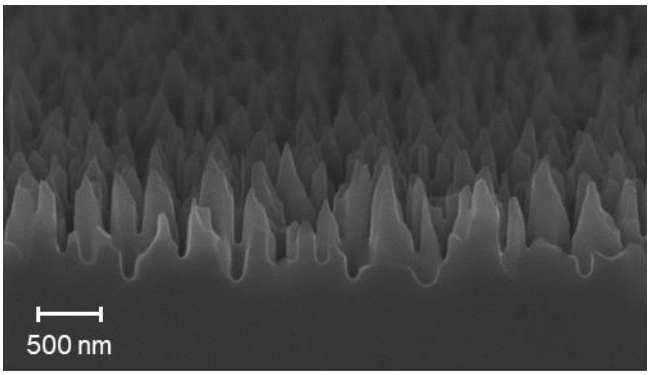

FIG. 2. An SEM micrograph of the b-Si nanostructure fabricated with ICP-RIE etching.

The exposure time in both light soaking and damp heat studies was cumulatively 1000 h. In light soaking, two quarters of each wafer were exposed to 0.6 sun illumination under an LED lamp on a hot plate at 75°C, while the remaining two quarters were stored in the dark as reference samples. Stability of the surface passivation was monitored during light soaking with PCD measurements on the reference samples as well as the light soaked samples at designated exposure intervals.

In the damp heat experiments, three quarters of one wafer were exposed to 85°C/85% relative humidity (RH), while one quarter was kept in ambient air at room temperature as a reference. Band-to-band photoluminescence (PL) imaging was used to monitor the stability of surface passivation at ~90 h exposure intervals. The PL light source consisted of blue, red and green LEDs filtered with a 1000 nm long pass filter with a total irradiance of 700 W/m^2 at the sample plane. PCD measurements could not be conducted during the damp heat exposure due to facility limitations, but as the PL signal and effective charge carrier lifetime are related[28], the methods are comparable for stability monitoring.

Finally, total charge Q_{tot} and interfacial defect density D_{it} of the passivation film were measured from exposed and reference planar samples using contactless CV (Corona Oxide Characterization of Semiconductor, COCOS)[29] with a Semilab SDI PV-2000A tool. All uncertainty values in PL intensity, Q_{tot} and D_{it} are evaluated as the standard deviation of multiple measurement results for each individual wafer quarter. Thus, they do not necessarily take variation between different wafers into account.

III. RESULTS AND DISCUSSION

Before light soaking and damp heat exposure, it was observed that τ_{eff} was dependent on the thickness of the passivation film in both b-Si and planar samples. For the respective film thicknesses, τ_{eff} in planar samples was always higher than in b-Si samples, similarly to our previous studies on the SALD passivation of b-Si[26]. This was expected due to the higher surface area of b-Si, leading to more recombination sites, and potential damage to the silicon lattice during the etching[30]. Samples with an AlO_x thickness of 20 nm yielded the highest initial lifetime in the range of 900 µs to 1000 µs

for b-Si and 1200 µs to 3000 µs for planar silicon, while for the samples with an AlO_x thickness of 5 nm the lifetime was approximately 370 µs to 580 µs for b-Si and 450 µs to 630 µs for planar. In accordance to this trend, the lifetime in the samples with an AlO_x thickness of 2 nm was significantly lower: approximately 30 µs to 75 µs for b-Si and 120 µs to 165 µs for planar samples. This effect can be attributed to both a reduction of overall field-effect passivation in the thinner films, and an increased density of defects due to a non-uniform surface coverage of the surface with the SALD film. Taking these initial observations into account, the impact of film thickness on the passivation stability under light soaking and damp heat exposure is considered in the subsections below.

A. Passivation Stability under Light Soaking

Figure 3(a) presents τ_{eff} at an excess carrier density of $1 \cdot 10^{15}$ cm^{-3} as a function of light soaking duration, with open symbols referring to b-Si samples and filled symbols to planar samples. Generally, the passivation quality was very stable under light soaking, and differences between b-Si and planar samples were minuscule. In both b-Si and planar samples passivated with the 20 nm thick AlO_x no drop in lifetime was observed throughout the 1000 h-long exposure. The lifetime in the samples with 5 nm thick AlO_x degraded only slightly. Initially, the lifetime in b-Si samples with 5 nm thick AlO_x was 580 µs, which dropped to approximately 410 µs after 1000 h of exposure. In the planar samples, the change was less pronounced, from 630 µs initially to 570 µs at 1000 h. The lifetime in the samples with 2 nm thick AlO_x had dropped significantly already after 1 h of light soaking: τ_{eff} decreased from 30 µs to 11 µs in b-Si samples and from 120 µs to 49 µs in planar samples. After this the lifetime in samples with 2 nm thick AlO_x remained at a similar level throughout the duration of the experiment. For b-Si and planar samples

with 2 nm films the change in lifetime occurred on comparable time-scales. Additionally, with 5 nm and 20 nm thick films there were no dramatic differences between b-Si and planar samples either, suggesting similar degradation kinetics for b-Si and planar surfaces. During light soaking, the decrease of lifetime in the 2 nm and 5 nm samples could not be explained by damage originating from sample handling during the measurements, as all reference samples were measured at the same intervals as the light-soaked samples, and the lifetime in the reference samples did not decrease.

Figure 3(b) shows the Q_{tot} and midgap D_{it} results for the planar light soaked samples after 1000 h of exposure (in red) and for the reference samples (in blue). Although measuring very thin oxide layers accurately with COCOS is difficult and measurement inaccuracies can affect the results, a systematic decrease of Q_{tot} and, therefore, loss of field effect passivation was observed in the light-soaked 2 nm samples compared to reference samples stored in the dark. This is in agreement with the results of Sperber *et al.*[16] However, the strongly decreased D_{it} of the 2 nm samples suggested improved chemical passivation after light soaking. As the minority carrier lifetime decreased in these samples, it seems that for 2 nm thick AlO_x layers field-effect passivation is a dominant mechanism over chemical passivation. For the 5 nm samples an opposite trend was observed, as the light-soaked samples exhibited a slightly higher negative charge compared to the reference samples. This is in line with the observations of Liao *et al.*[31], and a likely cause for this is the charging of the $Si/SiO_x/AlO_x$ interface under intense illumination due to carrier injection and trapping. Under the aforementioned assumption, the increase in field effect passivation should have led to increased lifetime, but an opposite trend was observed. D_{it} of the 5 nm samples did not

provide an explanation to the decrease in lifetime either, as values measured from the reference and the light soaked samples were at a similar level. The difference in Q_{tot} of the 20 nm samples was very small, almost within the uncertainty range, and in line with the stable lifetime throughout the experiment.

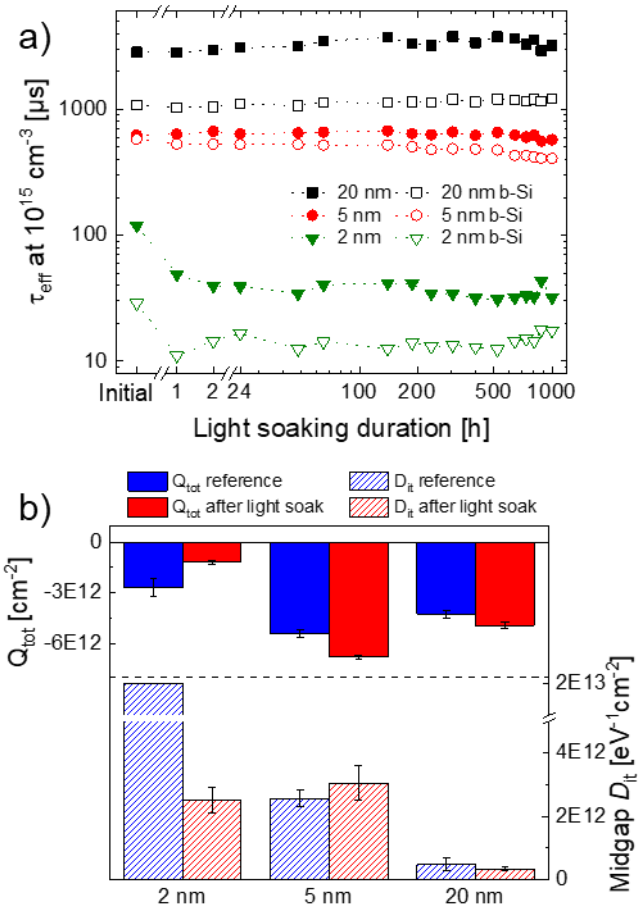

FIG. 3. (a) τ_{eff} as a function of light soaking duration and (b) Q_{tot} and midgap D_{it} results from reference samples and after light soaking. The open circles in figure (a) refer to b-Si samples, while the filled symbols denote a planar surface. Figure (b) shows the results only for planar substrates, as Q_{tot} and D_{it} could not be accurately determined from the b-Si samples.

B. Passivation Stability under Damp Heat Exposure

In general, the wafers exposed to damp heat showed more pronounced changes than the light soaked samples. However, the samples with 20 nm thick AlO_x remained remarkably stable even in the harsh 85°C/85% RH conditions. Minority carrier lifetime

results measured before and after damp heat exposure are presented in Figure 4(a). For the samples with 5 nm thick AlO_x the changes were pronounced: for b-Si samples the lifetime was initially 360 µs and after exposure 13 µs, while for planar samples the corresponding values were 490 µs and 90 µs. In the b-Si samples with 2 nm thick AlO_x τ_{eff} dropped from 75 to 6 µs, while for planar samples the lifetime dropped from 125 µs to 11 µs. Based on the lifetime results with 5 nm thick AlO_x, it seems that the extent of surface passivation degradation of b-Si samples was higher than in their planar counterparts, which can be explained with the higher surface area of black silicon. We speculate that the AlO_x-passivated b-Si structure had more area to react with the water vapor, leading to faster degradation of surface passivation properties. However, film thickness had a more significant impact on passivation stability compared to surface texture, as both b-Si and planar samples passivated with 20 nm of AlO_x demonstrated essentially no degradation.

Q_{tot} and D_{it} results of the damp heat tests are presented in Figure 4(b). For 20 nm samples the very small changes in both film charge and defect density were in line with the highly stable lifetime. For 5 nm passivation layers, D_{it} was similar in the damp heat exposed and reference wafers, but a notable reduction of film charge was observed. Therefore, reduced field-effect passivation during the damp heat exposure is the most likely degradation method for the SALD-passivated samples, . We also speculate that the loss of negative charge of the passivation film and the formation of AlO(OH) during damp heat exposure, as observed by Liang *et al.*[20,21], are interlinked. After exposure the 2 nm film showed a positive total charge in the order of $1 \cdot 10^{11}$ cm^{-2}, explaining the significant drop of lifetime due to dramatic loss of field-effect passivation. However,

while the contactless CV results from the 2 nm samples were consistent, their actual scale is not necessarily accurate due to charge-leakage through the very thin oxide. It should also be noted that the uncertainty values presented in the graphs were determined from the actual measurements, so they reflect the consistency of the obtained results.

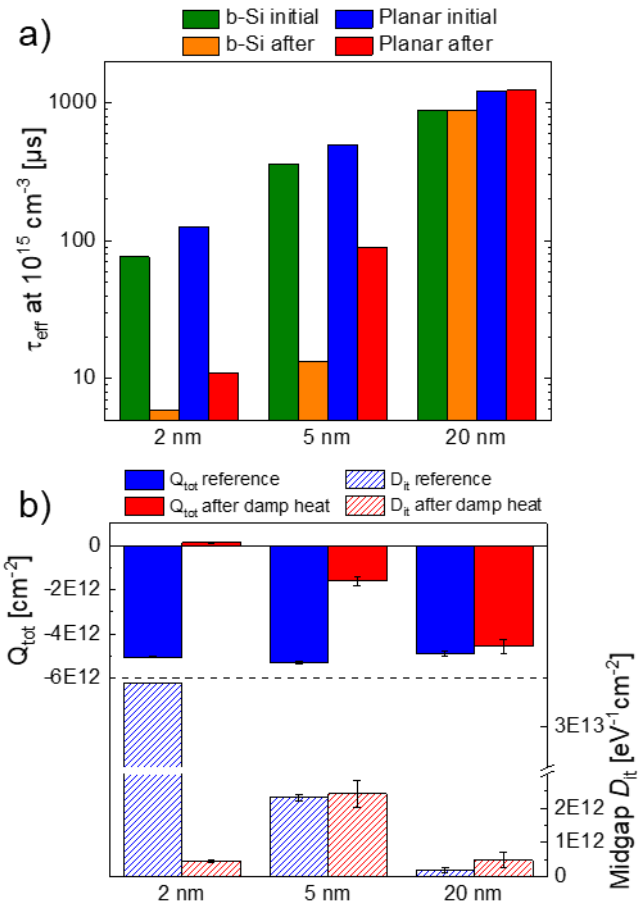

FIG. 4. (a) τ_{eff} and (b) Q_{tot} and midgap D_{it} results before and after 1000 h-long damp heat exposure. Again, Q_{tot} and D_{it} could be measured only on planar samples.

The PL signal intensity values extracted from photoluminescence images, shown in Figure 5(a), are in agreement with the lifetime results. Based on the monitoring measurements, the 20 nm passivation films were stable over the whole 1000 h long damp heat exposure. On the other hand, the PL signal obtained from the samples with 2 nm and 5 nm thick AlO_x layers deteriorated quickly with a notable decrease already after 100 h of

exposure. Samples with 5 nm thick AlO_x showed a steady gradual decrease in PL signal, while the signal obtained from the samples with 2 nm thick AlO_x was at the background level already after 100 h of exposure. In general, b-Si and planar samples behaved similarly, but the b-Si sample with 5 nm thick AlO_x degraded with a slightly stronger gradient with respect to ageing time than its planar counterpart. This indicates that the increased surface area of b-Si can increase the degradation rate in damp heat exposure. We speculate that the surface morphology influences the AlO_x quality so that b-Si samples with 5 nm thick AlO_x layers would have more pinholes in the surface than the planar ones, leading to faster degradation. However, the effect was not dramatic, as the surface texture did not influence the degradation rate of the 20 nm samples. Examples of the PL images of b-Si samples taken with identical parameters and presented with the same color scale are given in Figure 5(b). Both 5 nm and 20 nm samples showed a bright image (high PL signal) in the initial state, but after 500 h the signal from the 5 nm sample had noticeably decreased across the whole area of the sample. After 1000 h of exposure the image of the 5 nm samples was almost completely dark (low PL signal), while the 20 nm sample still showed a high PL signal.

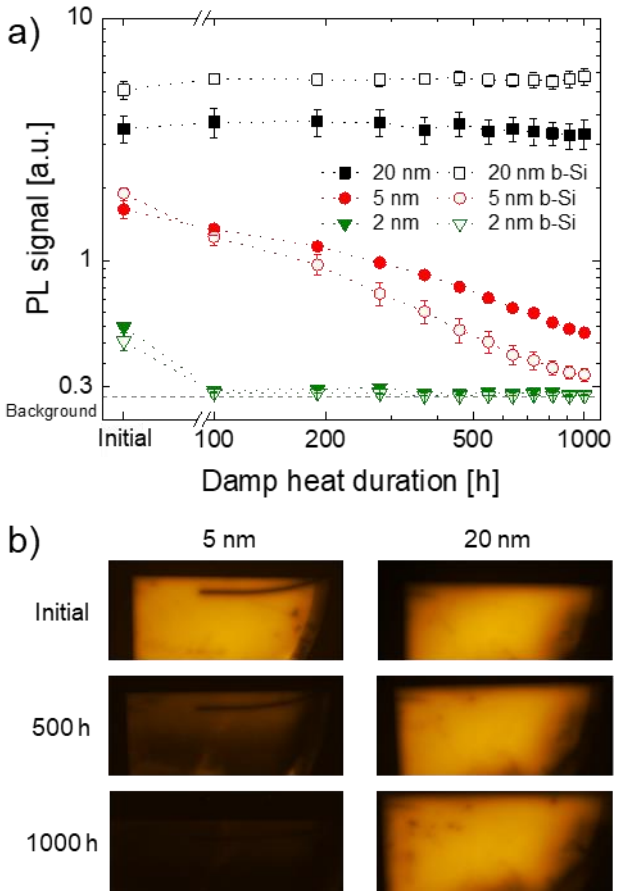

FIG. 5. (a) PL signal intensity as a function of damp heat exposure time. As previously, the open symbols are for b-Si and the filled symbols for planar samples. (b) PL images taken with identical measurement parameters of b-Si samples coated with 5 nm and 20 nm AlO_x in the initial state as well as after 500 h and 1000 h of damp heat exposure.

The SALD films here were less stable in damp heat conditions than films deposited with conventional ALD, as in our previous study we reported that even 5 nm ALD AlO_x passivation films were stable for up to 264 h in 85°C/85% RH[32]. A major difference between these studies is that the SALD tool used here was not located inside a particle-controlled cleanroom unlike the conventional ALD tool, which resulted in an increased particle level during the SALD passivation. Additionally, SALD films were potentially less dense than obtained with pulsing ALD, as the growth of SALD AlO_x is likely to contain a CVD-like component resulting from the intermixing of precursors

during deposition[22,23]. The initial Q_{tot} values between this study and the ones in our previous work[32] were comparable, so we speculate that the potential lower density of the film and an increased number of pinholes due to particles led to the accelerated degradation of Q_{tot} in the SALD films. However, 20 nm thick SALD AlO_x passivation films yielded highly stable passivation. In addition, for solar PV applications damp heat stress tests for bare wafers are already rather harsh tests, since encapsulation in PV modules will provide enough protection form high levels of moisture and oxygen.

C. Role of Interfacial Oxide

The interfacial SiO_x layer between the Si surface and the passivating film greatly influenced the passivation stability under both light soaking and damp heat exposure, at least in the case of 5 nm thick AlO_x films. The τ_{eff} monitoring results of samples with 5 nm thick AlO_x during light soaking are shown in Figure 6(a). The red symbols refer to samples with the SiO_x finish (open for b-Si, filled for planar) and the blue triangles to the planar HF-dipped sample, coated with 5 nm AlO_x as well. The HF-dipped sample initially showed a higher minority carrier lifetime than wafers with the SiO_x finish, which is not in agreement with results presented previously[33]. However, the SiO_x-finished b-Si and planar samples degraded slower than their HF-dipped counterpart. The lifetime of the HF-dipped sample decreased slowly from 850 µs to 510 µs until approximately 300 hours of exposure, after which the lifetime started to plummet, reaching 210 µs at 1000 h. The inset of Figure 6(a) shows the injection-dependent lifetime results of the HF-dipped sample, illustrating the gradual drop of lifetime at all injection levels throughout the exposure period. It can be seen in the inset figure that Shockley-Read-Hall recombination does not influence the lifetime at low injection levels in these samples, so it is clear that

the degradation is explained by an increase in surface recombination and not by a decrease in bulk lifetime[34]. Therefore, contamination resulting from the processing equipment is not a viable cause for the degradation in this case.

Similarly as in the light soaking case, the HF-dipped sample was less stable than the samples with SiO_x during damp heat exposure. However, the timescale of the degradation was quite different. Figure 6(b) shows the PL signal intensity of all the 5 nm samples at designated damp heat exposure intervals. The red circles, again, refer to the SiO_x samples and the blue triangles to the planar HF-dipped sample. The passivation quality of HF-dipped sample deteriorated quickly under damp heat, reaching a stable low value only slightly above the background level already after 100 h of exposure.

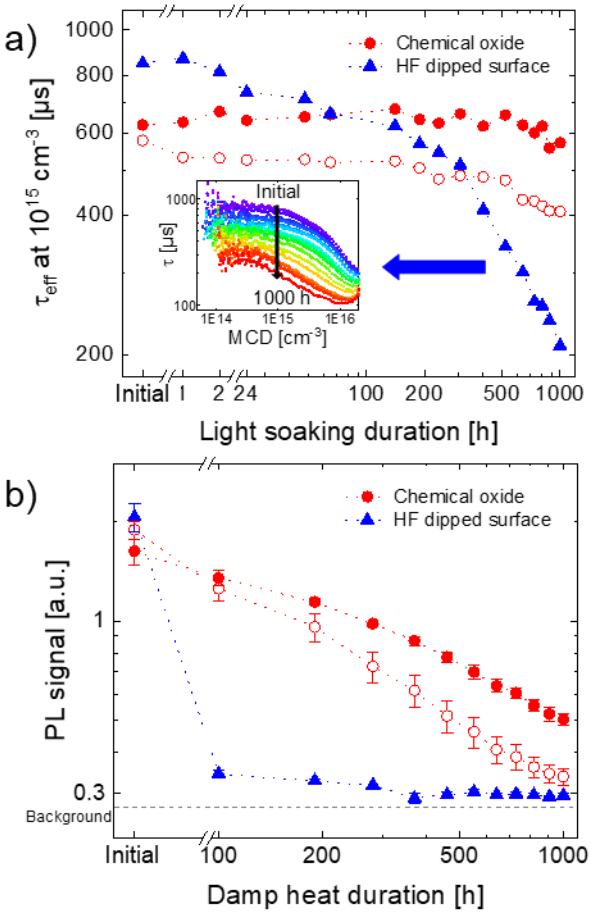

FIG. 6. (a) Lifetime throughout 1000 h of light soaking and (b) PL signal over the course of 1000 h damp heat exposure for SiO_x and HF-dipped 5 nm samples. Inset in Figure (a) shows the injection level dependent lifetime for HF-dipped samples over time. In both figures red circles refer to SiO_x samples (open symbols for b-Si, filled for planar), and blue triangles to planar samples that were HF-dipped prior to the deposition of 5 nm AlO_x.

Q_{tot} and D_{it} results, presented in Figure 7, similarly to the results above suggest that the reduction of lifetime under light soaking and damp heat occurred due to different degradation mechanisms. During damp heat exposure, the negative charge in the samples with SiO_x was reduced, whereas in the HF-dipped samples the initially negative charge had even turned positive with a value in the order of $1 \cdot 10^{10}$ cm^{-2}. Therefore, the extent of charge carrier lifetime degradation during damp heat exposure seems to be directly related to the loss of negative film charge. An interesting observation was that light soaking did not induce any significant changes in Q_{tot} or D_{it} regardless of the surface finish, leading to the conclusion that a different phenomenon led to the deterioration of lifetime in light soaking than under damp heat.

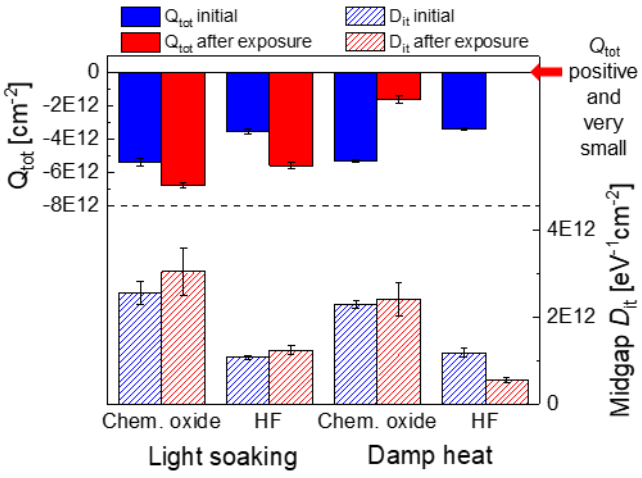

FIG. 7. Comparison of Q_{tot} and D_{it} results obtained from 5 nm planar samples with chemically-grown SiO_x and HF-dipped samples before and after light soaking and damp heat exposure.

The above result that degradation during damp heat exposure occurs due to reduction of field effect passivation is in agreement with the results reported by Liang *et al.*[20,21], but the root cause for the degradation under light soaking requires further studies. Sperber *et al.* have speculated that this can be induced by carrier-induced defects in silicon[17]. These defects would affect the lifetime more dramatically in the case of thinner passivation films, as the relatively low amount of charged film close to the silicon surface cannot compensate the effect of the defects on lifetime. The underlying defects causing surface related degradation in passivated silicon are likely located directly at the interface between the wafer and the passivating layers or very close to it[17,31], which is in agreement with the significance of the SiO_x layer in our studies. In this case, the chemically-grown SiO_x potentially suppresses the formation of these defect states close to the surface of silicon. The drastic differences between the stability of the SiO_x and HF-dipped samples suggest that the degradation during light soaking is truly related the interface between the passivation film and the silicon surface, and not to the film properties. As the SiO_x layer at the interface affects the degradation occurring during damp heat degradation, it seems that the mechanism behind the reduction of film charge is also related to the interplay between the substrate and the passivating film.

IV. CONCLUSIONS

AlO_x films deposited using industrially viable spatial ALD yield efficient and stable surface passivation even on nanostructured black silicon surfaces. We conclude that relatively thick passivation films (20 nm) are required to obtain high minority carrier lifetime that stays stable for over 1000 h under light soaking with 0.6 Sun illumination at 75°C or under damp heat exposure at 85°C/85% RH. 2 nm and 5 nm thick passivation

films showed degradation of effective lifetime in both environmental test conditions. During damp heat exposure, samples with 2 nm thick AlO_x layers degraded immediately, while the passivation quality obtained with 5 nm thick AlO_x films deteriorated slowly over time. This was attributed to reduced field effect passivation resulting from decreasing film charge. As the overall fixed charge density of the samples with 20 nm thick AlO_x was not significantly affected during damp heat exposure, it is possible that high ambient moisture only affects the top 2 nm to 5 nm of the passivation film. Light soaking studies showed a decrease in minority carrier lifetime which was not clearly explained by changes in film charge or interfacial defect density. A significant observation was that a thin chemically grown SiO_x layer remarkably enhanced passivation stability in both light soaking and damp heat exposure compared to samples that were HF-dipped prior to film deposition. This leads to the conclusion that degradation during light soaking is related to the interface between Si and the passivation layer, and that the interface plays a significant role in the reduction of fixed charge density in the AlO_x film during damp heat exposure as well.

The results of this study provide insights on the degradation mechanisms of surface passivation, which is highly relevant for the solar cell industry. Understanding the physical processes leading to degradation contribute to the development of more advanced passivation techniques with optimized film thicknesses. This study paves the way for using SALD in the industrial-scale production of highly stable optoelectronic components that rely on black silicon as the light absorbing surface.

ACKNOWLEDGMENTS

This work was funded through the European Metrology Programme for Innovation and Research (EMPIR) Project 16ENG03-HyMet. The EMPIR initiative is co-funded by the European Union's Horizon 2020 research and innovation programme and the EMPIR participating States. Additionally the Academy of Finland (PREIN Flagship Programme, decision No. 320165) is gratefully acknowledged. The authors acknowledge the provision of facilities by Aalto University at OtaNano – Micronova Nanofabrication Centre. NPL authors additionally acknowledge funding by the Department for Business, Energy and Industrial Strategy (BEIS) through the UK National Measurement System. Ismo T. S. Heikkinen acknowledges the financial support of Walter Ahlström foundation and Aalto ELEC Doctoral School. Michael Serué, Alisa Haukisalmi and Olli Setälä are thanked for their help with characterization and data analysis.

REFERENCES

[1]M. A. Juntunen, J. Heinonen, V. Vähänissi, P. Repo, D. Valluru, and H. Savin, Nat. Photon. **10**, 777-781 (2016).

[2]H. Savin, P. Repo, G. von Gastrow, P. Ortega, E. Calle, M. Garin, and R. Alcubilla, Nat. Nanotech. **10**, 624-629 (2015). Phys. **104**, 113703 (2008).

[4]R. S. Bonilla, B. Hoex, P. Hamer, P. R. Wilshaw, Phys. Status Solidi A **214**(7), 1700239 (2017).

[5]P. Repo, A. Haarahiltunen, L. Sainiemi, M. Yli-Koski, H. Talvitie, M. C. Schubert, and H. Savin, IEEE J. Photovolt. **3**(1), 90-94 (2013).

[6]G. von Gastrow, R. Alcubilla, P. Ortega, M. Yli-Koski, S. Conesa-Boj, A. Fontcuberta i Morral, and H. Savin, Sol. Energy Mater. Sol. Cells **142**, 29-33 (2015).

[7]Elfys Inc, "Technology", https://www.elfys.fi/index.php/technology/, 2019 (accessed 25 October 2019).

[8]PVTech, D. Ola, "GCL-SI hits 20.6% efficiency for its multicrystalline PERC solar cells", https://www.pv-tech.org/news/gcl-si-breaks-efficiency-record-with-20.6-for-its-multicrystalline-perc-sol, 2017 (accessed 25 October 2019).

[9]PVTech, M. Osborne, "Canadian Solar placing major bet on next-gen p-type multi cell technology", https://www.pv-tech.org/editors-blog/canadian-solar-placing-major-bet-on-next-gen-p-type-multi-cell-technology, 2017 (accessed 25 October, 2019).

[10]T. P. Pasanen, V. Vähänissi, F. Wolny, A. Oehlke, M. Wagner, M. A. Juntunen, I. T. S. Heikkinen, E. Salmi, S. Sneck, H. Vahlman, A. Tolvanen, J. Hyvärinen, and H. Savin, 35th European Photovoltaic Solar Energy Conference and Exhibition, EU PVSEC Proceedings, 552-556 (2018).

[11]D. Payne, T. H. Fung, M. U. Khan, J. Cruz-Campa, K. McIntosh, and M. Abbott, AIP Conf. Proc. **1999**, 050007 (2018).

[12]G. Dingemans, and W. M. M. Kessels, J. Vac. Sci. Technol. A **30**, 040802 (2012).

[13]P. Poodt, D. C. Cameron, S. M. George, V. Kuznetzov, G. N. Parsons, F. Roozeboom, G. Sundaram, and A. Vermeer, J. Vac. Sci. Technol. A **30**, 010802 (2012).

[14]F. Kersten, P. Engelhart, H.-C. Ploigt, A. Stekolnikov, T. Lindner, F. Stenzel, M. Bartzsch, A. Szpeth, K. Petter, J. Heitmann, and J. W. Müller, Sol. Energy Mat. Sol. Cells **143**, 83-86 (2015).

[15]D. Sperber, A. Herguth, and G. Hahn, Energy Procedia **92**, 211-217 (2016).

[16]D. Sperber, A. Schwarz, A. Herguth A, and G. Hahn, Sol. Energy Mat. Sol. Cells **188**, 112-118 (2018).

[17]D. Sperber, *Bulk and Surface Related Degradation Phenomena in Monocrystalline Silicon at Elevated Temperature and Illumination*, doctoral dissertation, University of Konstanz, Germany, 2019.

[18]T. Niewelt, W. Kwapil, M. Selinger, A. Richter, and M. C. Schubert, IEEE J. Photovolt. **7**(5), 1197-1202 (2017).

[19]K. Kim, R. Chen, D. Chen, P. Hamer, A. Ciesla nee Wenham, S. Wenham, and Z. Hameiri, IEEE J. Photovolt. **9**(1), 97-105 (2019).

[20]W. Liang, K. J. Weber, D. Suh, J. Yu, J. Bullock, IEEE 39th Photovoltaic Specialists Conference (PVSC) Part 2 (2013) 038-044.

[21]W. Liang, D. Suh, J. Yu, J. Bullock, K.J. Weber, Phys. Status Solidi A 212(2) (2015) 274-281. https://doi.org/10.1002/pssa.201431256.

[22]D. Pan, T.-C. Jen, C. Yuan, Int. J. Heat Mass Transf. 96 (2016) 189–198. https://doi.org/10.1016/j.ijheatmasstransfer.2016.01.034.

[23]D. Pan, Int. J. Heat Mass Transf. 144 (2019), 118642. https://doi.org/10.1016/j.ijheatmasstransfer.2019.118642.

[24]N.E. Grant, V.P. Markevich, J. Mullins, A.R. Peaker, F. Rougieux, D. Macdonald, Phys. Status Solidi RRL 10(6) (2016) 443-447. https://doi.org/10.1002/pssr.201600080.

[25]M.L. Green, M.-Y, Ho, B. Busch, G.D. Wilk, T. Sorsch, T. Conard, B. Brijs, W. Vandervorst, P.I. Räisänen, D. Muller, M. Bude, J. Grazul, J. Appl. Phys. 92 (2002), 7168. https://doi.org/10.1063/1.1522811.

[26]I.T.S Heikkinen, P. Repo, V. Vähänissi, T. Pasanen, V. Malinen, H. Savin, Energy Procedia 124 (2017) 282-287. https://doi.org/10.1016/j.egypro.2017.09.300.

[27]R.A. Sinton, A. Cuevas, Appl. Phys Lett. 69 (1996), 2510. https://doi.org/10.1063/1.1416134.

[28]T. Trupke, B Mitchell, J.W. Weber, W. McMillan, R.A. Bardos, R. Kroeze, Energy Procedia 15 (2012) 135-146. https://doi.org/10.1016/j.egypro.2012.02.016.

[29]M. Wilson, J- Lagowski, L. Jastrzebski, A. Savtchouk, V. Faifer, AIP Conf. Proc.550 (2001) 220-225. https://doi.org/10.1063/1.3021091.

[30]G. Kumaravelu, M.M. Alkaisi, A. Bittar, D. Macdonald, J. Zhao, Curr. Appl. Phys 4 (2004) 108-110.

[31]B. Liao, R. Stangl, T. Mueller, F. Lin, C.S. Bhatia, B. Hoex, J. Appl. Phys. 113 (2013), 024509. https://doi.org/10.1063/1.4885096.

[32]I.T.S. Heikkinen, G. Koutsourakis, S. Wood, V. Vähänissi, F.A. Castro, H. Savin, AIP Conf. Proc. 2147 (2019), 050003. https://doi.org/10.1063/1.5123852.

[33]Y. Bao, S. Li, G. von Gastrow, P. Repo, H. Savin, M. Putkonen, J. Vac. Sci. Technol. A 33(1) (2015), 01A123-1. https://doi.org/10.1116/1.4901456.

[34]D. Schröder IEEE T. Electron Dev. 44(1) (1997) 160-170.